Proceedings of the 18th World Congress
The International Federation of Automatic Control
Milano (Italy) August 28 - September 2, 2011

Design and Experimental Validation of an Explicit MPC Controller for Regulating Temperature in PEM Fuel Cell Systems

Alicia Arce * **Christos Panos** ** **Carlos Bordons** *
Efstratios N. Pistikopoulos **

* *Automation and System Engineering Department, University of Seville, 41092 Sevilla, Spain. (e-mail: aarce@cartuja.us.es, bordons@esi.us.es).*
** *Centre of Process Systems Engineering. Department of Chemical Engineering, Imperial College London, London. (e-mail: christos.panos08@imperial.ac.uk, e.pistikopoulos@imperial.ac.uk)*

Abstract:
This paper proposes a temperature controller for PEM fuel cell systems with an air blower as thermal circuit. The objective of this controller is to maintain the stack temperature over a given set-point which is obtained from the results of a real-time optimization algorithm with the goal of minimizing the stack degradation and maximizing the global efficiency. An Explicit MPC is proposed to deal with this control problem which presents delays, the critical sampling time, constraints and disturbances. The simulation results show good performance of the controller which accurately tracks the temperature reference over the overall range of operating conditions. Furthermore, the controller is implemented in real-time on a PEM fuel cell test-bench which is installed in the Fuel Cell Laboratory at the University of Seville.

Keywords: Real-time, model predictive and optimization-based control, optimal operation and control of power systems.

1. INTRODUCTION

PEM (Polymeric Electrolyte Membrane) Fuel cells are devices which generate electric energy by combining hydrogen and oxygen through a polymeric membrane and produce water and heat. The low operating temperature and the fast start-up make this kind of fuel cells suitable for stationary and mobile applications. Currently this technology has been considerably developed but there are some drawbacks such as durability and production costs that need to be overcome in order to be competitive with conventional technologies. Thus, the application of advanced control techniques in order to improve efficiency and lifetime is justified.

This paper studies the influence of the stack temperature on the fuel cell performance and net power generation and then proposes an advanced controller in order to regulate the air cooling system. As previously mentioned, normal operation of the fuel cell system relies on an exothermic reaction, which has the effect of increasing the temperature of the fuel cell. As the stack temperature rises, so does the rate of reaction, which in turn results in an increase in net power generation and the overall efficiency of the fuel cell. However, excessive increases of fuel cell temperature result in the degradation of the membrane and the fuel cell stack due to thermal stress and degradation. Ultimately, a compromise between degradation and efficiency must be obtained in order to appropriately control the operation of the fuel cell.

⋆ This work was supported by Spanish Ministry of Science and Innovation under grant DPI2008-05818.

The thermal dynamics plays an important role in the fuel cell performance. The work presented in Schmittinger and Vahidi (2008) shows that the operating temperature significantly influences on the water content inside the fuel cell. Therefore a low operating temperature causes a high water content which results in flooding of the anode channel Mckay et al. (2008) and reduces the fuel cell lifetime. Conversely, if the operating temperature is very high, the membrane becomes dehydrated which results in an increase in the rate of stack degradation. The authors conclude that there is an optimal range of water content that minimizes the degradation which corresponds to an optimal stack temperatures that will be the reference for the dynamic controller, see Arce et al. (2011).

In the literature, the majority of previous contributions design and analyze air feed regulators which is as important as the temperature controller. Some authors Riascos and Pereira (2009), Binrui et al. (2009), Ahn and Choe (2008) and Mor et al. (2010) propose temperature controllers based on PID-controllers (Proportional Integral Derivative controller). Specifically, Riascos and Pereira (2009) presents a PI-controller with small gains, Binrui et al. (2009) develops a fuzzy incremental PID control algorithm, Ahn and Choe (2008) compares the results of a classic PI-controller with a state feedback controller and Mor et al. (2010) proposes a PI-controller with anti-windup. The work published in Na and Gou (2008) designs a feedback loop with disturbance compensator. In addition, the works presented in Riascos and Pereira (2009) and Binrui et al. (2009) include a generator of optimal temperature references based on the air humidity and load profile respectively. To the best of our

knowledge, none of these papers designs an advanced controller which is capable of dealing with physical constraints, disturbances and delays simultaneously while future reference predictions are accounted for in order to improve the control performance and at the same time present experimental validation. To this end, this work focuses on the advanced control design and the study of the real-time implementation. Thus, it is proposed an Explicit MPC (Model Predictive Control) controller Bemporad et al. (2002) which includes feedforward effects to take disturbances into account and physical constraints, predicts the temperature profile to overcome the delays and reduces the execution time making the solution of this control problem feasible for real-time implementation. Moreover, the controller is implemented in real-time and the control performance is empirically validated. Otherwise, the set-points are obtained by a real-time optimization algorithm based on the water content which minimizes the degradation rate and maximizes the global efficiency as presented in Arce et al. (2011). This optimization is not herein described because it is not the scope of this work.

The paper is organized as follows: Section 2 describes the fuel cell system which is modeled. In Section 3, the non-linear model used for the control design and simulation validation is presented. Section 4 shows the discrete linear model for control design. Sections 5 and 6 present the control formulation and the simulation results respectively. In Section 7 the controller is implemented in real-time and the simulation results are validated with real data. Finally, we present our conclusions in Section 8.

2. SYSTEM DESCRIPTION

The work presented in this paper is based on a 1.2 kW Ballard PEM fuel cell (Nexa Power Module) which is installed in the laboratory at the University of Seville. This apparatus is currently in use by many research groups and considered to be the state of the art in PEM technology.

The stack comprises 46 cells, each with a 110 cm^2 membrane. The system is auto-humidified and air–cooled by a small fan which consumes as a maximum over 100 W. Hydrogen was fed to the fuel cell in dead-end mode, with flushing. Figure 1 shows the real fuel cell system which is installed in the laboratory of the University of Seville.

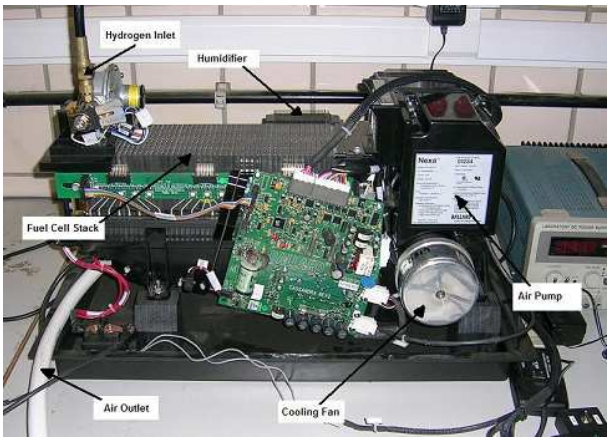

Fig. 1. 1.2 kW Nexa power module

3. NON-LINEAR PEM FUEL CELL MODEL

The model which is used for simulating and validating the controller is semi-empirical, i.e., it comprises first principles and empirical relationships and zero-dimensional. This model published in del Real et al. (2007) includes two-phase fluid dynamics considering flooding phenomenon, heat transfer dynamics and algebraic formulation of the polarization curve.

The thermal equations are summarized in this section in order to understand the non-linear model of the stack temperature. The physical parameters have been experimentally obtained from the data of the bed-test. An energy balance is performed in order to obtain the thermal model, accounting for the energy rate produced in the chemical reaction of water formation (which is supposed to be formed as water vapor), $\dot{H}_{reac}$, the power supplied in the form of electricity, P_{st}, and the amount of heat evacuated by radiation, $\dot{Q}_{rad,FC2amb}$, and both natural and forced convection, $\dot{Q}_{conv,FC2amb}$. Heat removal is completed through forced convection by a small fan. In bigger fuel cell stack systems, where the amount of heat is considerably larger, water cooling is necessary. In those cases, the forced convection term should be substituted by other terms which model heat exchange in cooling fluid. The energy balance results in:

$$m_{st} \cdot C_{st} \cdot \frac{dT_{st}}{dt} = \dot{H}_{reac} - P_{st} - \dot{Q}_{rad,FC2amb} - \dot{Q}_{conv,FC2amb} \quad (1)$$

The stack temperature is measured by a thermistor which can be modeled by a first-order approximation with a time constant of 10 seconds.

$$\tau \cdot \frac{dT^*_{st}}{dt} + T^*_{st} = T_{st} \ , \quad (2)$$

where T^*_{st} is the temperature measured by the thermistor and τ is the time constant of the thermistor.

Regarding air cooling, a small fan is used to supply the cooling air flow. The heat transfer dynamics of the fuel cell are several magnitude orders slower than the fluid-dynamics associated with the cooling air flow, therefore, the last ones are neglected in our model. Moreover, the amount of air supplied by the fan can be considered as linearly proportional to the control signal of the fan. In this way, the equation that links the fan voltage, V_{fan}, between 0 and 100 (%), with the air flow supplied expressed in kg s^{-1}, $\dot{m}_{cool}$, is given by:

$$\dot{m}_{cool} = 36 \cdot V_{fan} \ . \quad (3)$$

This model was successfully validated with experimental data gathered from the Nexa Power module as shown in del Real et al. (2007).

4. DISCRETE LINEAR MODEL

A discrete linear model is obtained by simplifying the non-linear model presented in Section 3. This model generates stack temperature predictions which are involved in the minimization of the cost function performed by the Model Predictive Controller (MPC). The thermal linear model has as input the fan voltage, V_{fan}, and as output the stack temperature, T_{st}. Moreover, this model has two disturbances which are the load current, I_{st}, and the ambient temperature, T_{amb}, which is assumed to be equal to the temperature of the cooling air. Figure 2 shows the scheme of the linear model where the input, output and disturbances are represented.

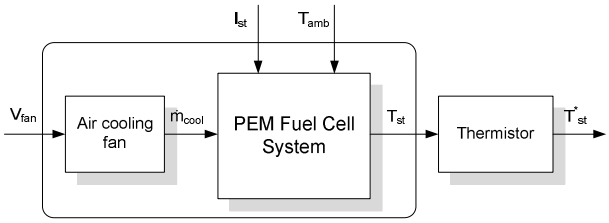

Fig. 2. Discrete Linear Model Scheme

The choice of a suitable sampling time is an important task. Analyzing the heat transfer dynamics, the characteristic time of the fuel cell temperature without the dynamic of the thermistor is 800 ms. However, including the thermistor in the analysis, the characteristic time of the system is 10s and thus, a sampling time of 400 ms is chosen.

The fuel cell linear model is obtained by linearizing the model presented in Section 3 over an operation point. The operation point chosen for the linearization is 20 A of load current, 300 K of ambient temperature and $47°C$ of stack temperature. Moreover, the non-linear model includes the oxygen excess ratio controller previously published in Arce et al. (2009). The linearization results in a state-space model which comprises 12 state variables ($\mathbf{x}$), one input (u), two disturbances ($\mathbf{v}$) and one output (y). The continuous linear model is simplified and represented by the following matrices:

$$\begin{aligned} \dot{\mathbf{x}} &= A\cdot\mathbf{x} + B\cdot \mathrm{u} + D\cdot\mathbf{v} \\ \mathrm{y} &= C\cdot\mathbf{x}\,, \end{aligned} \tag{4}$$

where

$$A = \begin{bmatrix} -24.41 & 22.13 & 16.78 & 3.912 \\ 2045 & -2394 & -1442 & -284.6 \\ -44.24 & 136.9 & 75.35 & 13.12 \\ -176.7 & 64.14 & 37.48 & 6.57 \end{bmatrix},$$

$$B = \begin{bmatrix} 3.293\ 10^{-6} \\ 5.035\ 10^{-6} \\ 0.001076 \\ -0.00207 \end{bmatrix},$$

$$D = \begin{bmatrix} -6.72\ 10^{-6} & -0.0002267 \\ -9.851\ 10^{-6} & 0.02499 \\ -0.002114 & 0.00281 \\ 0.004069 & -0.008808 \end{bmatrix},$$

$$C = [\,-0.001411\ \ -0.002158\ \ -0.461\ \ 0.8873\,]\,.$$

Discretizing the previous model (4), the discrete linear model is:

$$\begin{aligned} \mathbf{x}(k+1) &= A_d\cdot\mathbf{x}(k) + B_d\cdot\mathrm{u}(k) + D_d\cdot\mathbf{v}(k) \\ \mathrm{y}(k) &= C_d\cdot\mathbf{x}(k)\,, \end{aligned} \tag{5}$$

$$A_d = \begin{bmatrix} 0.8669 & 0.0157 & 0.1164 & 0.0396 \\ -0.2852 & -0.0287 & -0.4364 & -0.0420 \\ 2.5934 & 0.0772 & 0.9564 & -0.0436 \\ -4.4219 & -0.0369 & -0.3458 & 0.8545 \end{bmatrix},$$

$$B_d = \begin{bmatrix} 0.0011\ 10^{-3} \\ -0.0155\ 10^{-3} \\ 0.0441\ 10^{-3} \\ -0.0837\ 10^{-3} \end{bmatrix},$$

$$D_d = \begin{bmatrix} -0.0022\ 10^{-3} & 0.0038\ 10^{-3} \\ 0.0305\ 10^{-3} & -0.0506\ 10^{-3} \\ -0.0867\ 10^{-3} & 0.1726\ 10^{-3} \\ 0.1645\ 10^{-3} & -0.3279\ 10^{-3} \end{bmatrix},$$

$$C_d = [\,-0.001411\ \ -0.002158\ \ -0.461\ \ 0.8873\,]\,.$$

The system output (y) is the stack temperature, T_{st}, the input (u) is the fan voltage, V_{fan}, and the disturbance vector is equal to $[I_{st}\ T_{amb}]^T$.

5. EXPLICIT MPC FORMULATION

The next step involves the design of a multi-parametric (mp) Model Predictive Controller for the PEM fuel cell system shown in Figure 1. The Model Predictive Control (MPC) solves an open-loop optimal control problem at regular intervals (sampling time) in order to obtain a sequence of the current and future control actions up to a certain time horizon (in a receding horizon control fashion), given the current process measurements and based on the future predictions of the outputs and/or states obtained by using a mathematical representation of the system. Only the first input of the control sequence is applied to the system and the procedure is repeated at the next time instant when the new data are available. Being an on-line constrained optimization method, MPC not only provides the maximum output of a cost function but also takes into account the various physical and operational constraints of the system. In this work, a nominal mp-MPC controller is designed as presented in Bemporad et al. (2002), based on the linear state-space model obtained in the previous section by considering A_d, B_d, D_d and C_d as constant matrices. The following MPC formulation is considered for the PEM fuel cell system:

$$\begin{aligned} \min_{\mathrm{x,u,y}} \sum_{k=1}^{N_y-1} &\left[(\mathrm{y}_k - \mathrm{y}_{ref,k})^T\cdot Q\cdot(\mathrm{y}_k - \mathrm{y}_{ref,k})\right] + \\ &+ \sum_{k=1}^{N_u-1} \left[(\mathrm{u}_k - \mathrm{u}_{ref,k})^T\cdot R\cdot(\mathrm{u}_k - \mathrm{u}_{ref,k})\right] + \\ &+ (\mathrm{y}_{N_y} - \mathrm{y}_{ref,N_y})^T\cdot P\cdot(\mathrm{y}_{N_y} - \mathrm{y}_{ref,N_y})\,, \end{aligned} \tag{6}$$

subject to

$$\begin{aligned} \mathbf{x}(k+1) &= A_d\cdot\mathbf{x}(k) + B_d\cdot\mathrm{u}(k) + D_d\cdot\mathbf{v}(k)\,, \\ \mathrm{y}(k) &= C_d\cdot\mathbf{x}(k)\,, \\ \mathrm{y}_{min} &\le \mathrm{y}(k) \le \mathrm{y}_{max}\,, \\ \mathrm{u}_{min} &\le \mathrm{u}(k) \le \mathrm{u}_{max}\,, \\ \mathbf{v}_{min} &\le \mathbf{v}(k) \le \mathbf{v}_{max}\,, \end{aligned}$$

where u is the manipulated variable, y is the controlled variable, y_{ref} is the optimal temperature profile, u_{ref} is the input reference profile, N_y is the prediction horizon and N_u the control horizon ($N_y = 10$, $N_u = 2$). The optimization problem involves two optimization variables u_k, u_{k+1} and six parameters $x_p = [x(1)_k\ \ x(2)_k\ \ x(3)_k\ \ x(4)_k\ \ v(1)_k\ \ v(2)_k\ \ \mathrm{y}_{ref,k}]^T$ which correspond to the states ($\mathbf{x}$), the two measurable disturbances (ambient temperature and stack current) and the temperature setpoint. The objective function is set to minimize the quadratic norm of the error between the output and its optimal profile while the constraints on u, $\mathbf{v}$ and y are also introduced. Particularizing the physical constraints are:

$$
\begin{aligned}
300\ K \leq\ T_{st}\ &\leq 333\ K\ , \\
0 \leq V_{fan}\ &\leq 100\ , \\
0 \leq\ I_{st}\ &\leq 40\ A\ , \\
290\ K \leq T_{amb}\ &\leq 305\ K\ .
\end{aligned}
$$

For the case of constant system matrices, the optimization problem is a multi-parametric Quadratic Programming (mp-QP) problem and can be solved with standard multi-parametric programming techniques published in Pistikopoulos et al. (2002). In our study, Parametric Optimization Software was used (see work presented in Ltd (2003)) to obtain the explicit controller description, which is the optimal map of the control variables as function of the parameters of the system. This optimal map consists of 229 critical regions and the corresponding control laws for the temperature controller. Each critical region is described by a number of linear inequalities $A_i \cdot \mathbf{x} \leq b_i$ and its corresponding control action $\mathrm{u} = K_i \cdot \mathbf{x} + c_i$, where i is the index of solutions.

Figure 3 shows the temperature control scheme which comprises three blocks: temperature reference generator, water content observer and temperature local controller. Note that the water content observer and the temperature reference generator are included in the scheme but they are not presented in the current work. The water content, m_l, is estimated by a closed-loop observer which is a function of the voltage drop, stack temperature and the stack current. Further, the temperature reference generator calculates the temperature set-point in order to maintain the water content over a values which minimize the membrane degradation and to simultaneously maximize the stack net power.

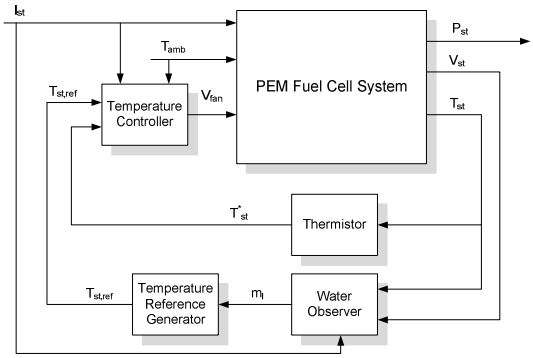

Fig. 3. Control architecture

6. SIMULATION RESULTS

In this section, the simulation results of the local controller are presented and discussed. The fuel cell is simulated including the oxygen excess ratio controller which was published in Arce et al. (2009). This controller has been implemented in real-time and validated with experimental data. The control objective is to track the oxygen excess ratio, λ_{O_2}, which is a variable related to the starvation phenomenon. The oxygen excess ratio is estimated by an observed which is a function of the stack temperature measured, T^*_{st}, the air flow which enters into the cathode, $\dot{m}_{ca,in}$, and the load current, I_{st}. Moreover, the oxygen excess ratio reference, $\lambda_{O_2,ref}$, is calculated by a reference generator which interpolates a curve obtained off-line by an optimization algorithm. The optimal oxygen excess ratio depends on the load current and stack temperature. Furthermore, the controller is an explicit MPC controller which includes disturbances and physical constraints, and the execution time is short enough to make this controller feasible for real-time implementation as it was demonstrated in Arce et al. (2009). Regarding the remaining actuators, the hydrogen valve is regulated by a proportional controller whose objective is to keep constant the anode pressure and the purge valve control is a heuristic controller which opens the valve when the voltage drop measured corresponds to a certain amount of water.

Figure 4 shows the global control scheme where the oxygen excess ratio control loop and the temperature control loop are represented in detail. The disturbances of each controller are clearly shown. As can be seen, the input of the controlled fuel cell system is the current demanded by the electronic load and the output is the net stack power supplied by the fuel cell. Due to the fact that the simulation results are focused on the performance of the temperature controller and the feasibility of the real-time implementation, the temperature optimization is not included in the simulations which will be studied in future works.

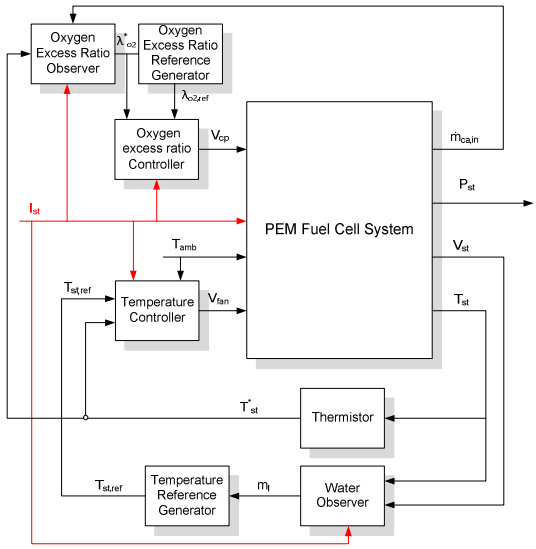

Fig. 4. Control of the fuel cell system scheme

6.1 Load current effects

The effect of the load current variation is analyzed. Figure 5 shows the load current profile simulated. Note that the ambient temperature is kept constant (27°C) for the entire simulation and the load current is varied from 15 A to 30 A.

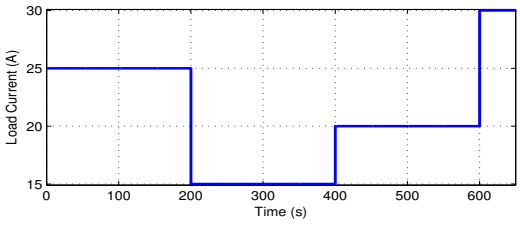

Fig. 5. Disturbances simulated

The performance of the controller is presented in Figure 6 where the stack temperature and the fan voltage are represented.

The control suitably tracks the reference as can be seen in the figure. The effects of the load current are observed on the fan voltage action which increases for higher currents and decreases for lower currents because the increment of current demand generates more heat that has to be removed. Moreover, the influence of the purge valve are observed as well. The purges decrease the stack temperature due to fact that the evacuation of hydrogen removes heat.

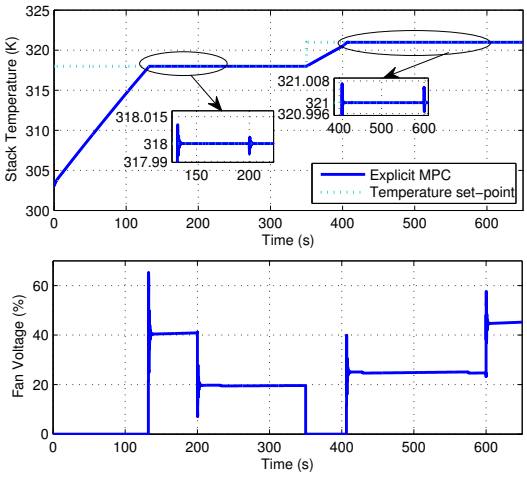

Fig. 6. Control performance simulated with load current variation

6.2 *Ambient temperature effects*

The air which is used to cool the stack down by the fan is at the same temperature of the ambient. For this reason, the ambient temperature influences on the heat transfer dynamics. For the same conditions as the simulation previously presented, the fuel cell stack needs more air in order to maintain the same stack temperature when the ambient temperature is higher. In Figure 7, the effects of the ambient temperature on the control action are observed. The ambient temperature is varied from 25° C to 30° C. As noted, the control performance is good, the reference is perfectly tracked and also there is not steady-state error.

6.3 *Execution time*

The execution time is an important variable which makes the control technique proposed feasible for real-time implementation. The advantage of the explicit formulation against the conventional model predictive control formulation is that the optimization is performed off-line and thus, the control executes a search for the optimal region every sampling time. However, if the number of regions is very high, the execution time might be not short enough for certain applications. In Figure 8, the execution time resulting of the simulation presented in Figure 7 is shown. The maximum execution time is equal to 2.5 ms and the average is 0.4 ms. The results has been obtained by simulating the controller in a PC of 2 Gb of RAM and core duo CPU of 1.6 GHz. The execution time can be shorter if the controller is implemented in a real-time platform. Note that, the execution time is 100 magnitude orders shorter than the sampling time, 400 ms, and it can be concluded that this proposal is feasible for real-time implementation.

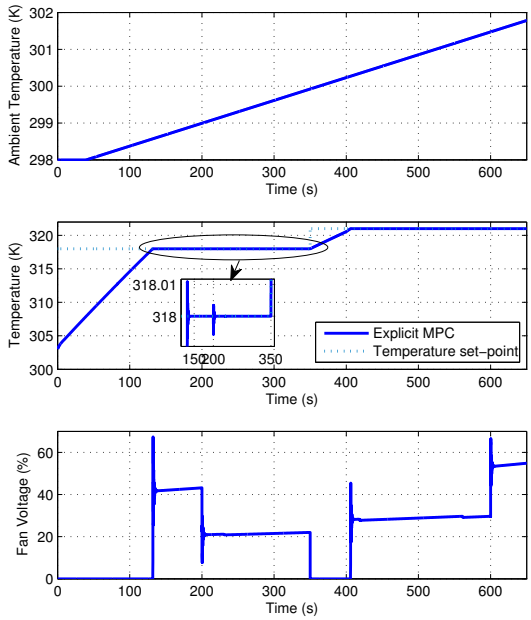

Fig. 7. Control performance with ambient temperature variation

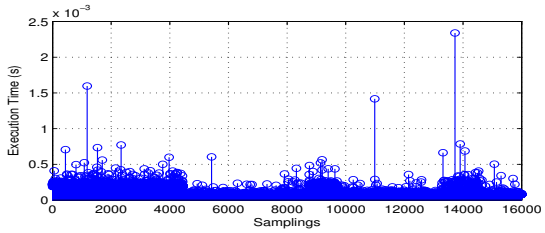

Fig. 8. Execution time

7. REAL-TIME IMPLEMENTATION

The experimental validation of the control proposed is presented in this section. Figure 9 shows the sensor equipment and the PC104 platform incorporated to the system to implement the control laws. A data acquisition card is also installed in order to gather and monitor the data obtained from the sensor net. Note that 'T1' and 'T2' are temperature sensors; 'V1', 'V2' and 'V3' are voltage sensors; 'C', 'C1' and 'C2' are current sensors; 'F' is a flow sensor; and 'P' is a pressure sensor.

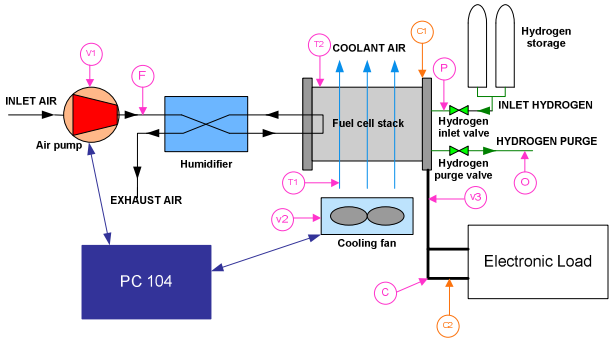

Fig. 9. Fuel cell system scheme

Figure 10 presents a picture of the industrial computer installed on the bed-test. The controller is implemented on the PC-104 by the Real-Time Workshop toolbox of Matlab^{TM}.

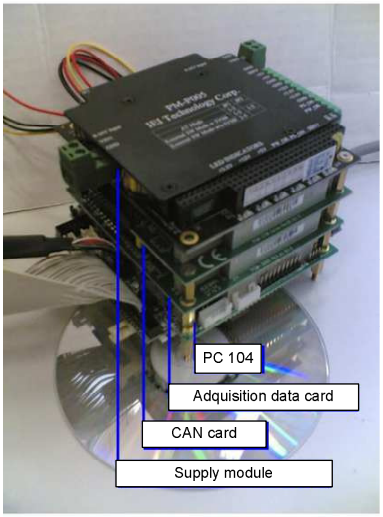

Fig. 10. Industrial PC platform incorporated to the test-bench

During the testing, the set-point is varied as shown in Figure 11. The ambient temperature increases with the fuel cell operation and the load current is kept constant in order to analyze the performance of the controller. The results of the experiments were successful and the temperature measured by the thermistor tracked the set-point indicated to the explicit controller. The temperature has a fast response without overshoot and there no steady-state error is observed.

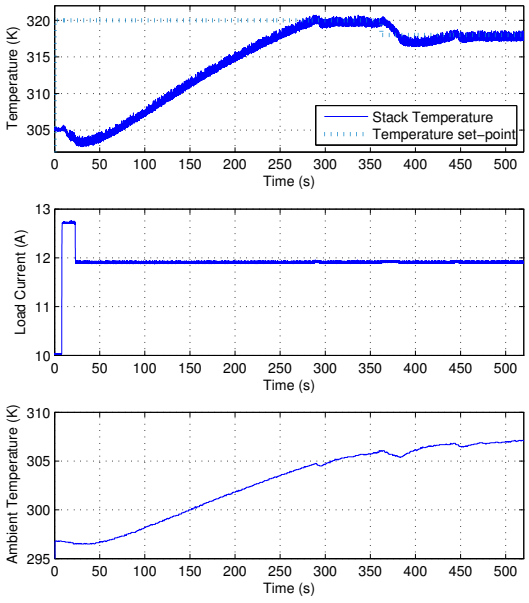

Fig. 11. Experimental validation of the temperature control

8. CONCLUSIONS

This paper has presented the design of an Explicit MPC controller in order to regulate the stack temperature of a PEM fuel cell system. The explicit MPC obtained comprised of 4 states, 2 disturbances, 1 input and 1 output, the number of regions is 460 and the control and predictions horizons are 2 and 10 respectively. Simulation and experimental results show that the control performance is suitable for real-time implementation and validate that the control proposal successfully deals with time delays, constraints and disturbances. However, many issues are opened such as the validation of the temperature reference optimization and the fuel cell operation with ambient temperature below zero.

ACKNOWLEDGEMENTS

The authors would like to thank Kostas Kouramas, Alejandro J. del Real and Alejandro Oliva for their help and support.

REFERENCES

Ahn, J.W. and Choe, S.Y. (2008). Coolant controls of a PEM fuel cell system. *Journal of Power Sources*, 179, 252–264.

Arce, A., Bordons, C., and del Real, A.J. (2011). Water management in PEM fuel cells: Controllability analysis and steady-state optimization for temperature control. In *Proceedings of the 18th IFAC World Congress*, in press.

Arce, A., Alejandro J. del Real, C.B., and Ramirez, D.R. (2009). Real-time implementation of a constrained MPC for efficient airflow control in a PEM fuel cell. *IEEE Transactions on Industrial Electronics*. 10.1109/TIE.2009.2029524.

Bemporad, A., Morari, M., Dua, V., and Pistikopoulos, E.N. (2002). The explicit linear quadratic regulator for constrained systems. *Automatica*, 38, 3–20.

Binrui, W., Yinglian, J., Hong, X., and Ling, W. (2009). Temperature control of PEM fuel cell stack application on robot using fuzzy incremental PID. In *Proceedings of 2009 Chinese Control and Decision Conference*, 3293–3297.

del Real, A.J., Arce, A., and Bordons, C. (2007). Development and experimental validation of a PEM fuel cell dynamic model. *J. Power Sources*, 173, 310–324.

Ltd, P.O.S.P. (2003). *Parametric Optimization Programming (POP) Toolbox*.

Mckay, D.A., Siegel, J.B., Ott, W., and Stefanopoulou, A.G. (2008). Parameterization and prediction of temporal fuel cell voltage behavior during flooding and drying conditions. *Journal of Power Sources*, 178, 207–222.

Mor, J., Puleston, P., Kunusch, C., and Visintin, A. (2010). Temperature control of a PEM fuel cell test bench for experimental MEA assessment. *Journal of Hydrogen Energy*. Doi:10.1016/j.ijhydene.2009.12.095.

Na, W. and Gou, B. (2008). A thermal equivalent circuit for PEM fuel cell temperature control design. In *Proceedings of 2008 IEEE International Symposium on Circuits and Systems*, 2825–2828.

Pistikopoulos, E., Dua, V., Bozinis, N., Bemporad, A., and Morari, M. (2002). On-line optimization via off-line optimization tools. *Journal of Computers and Chemical Engineering*, 26, 175–185.

Riascos, L.A. and Pereira, D.D. (2009). Optimal temperature control in PEM fuel cells. In *Proceedings of 35th Annual Conference of IEEE Industrial Electronics*, 2778–2783.

Schmittinger, W. and Vahidi, A. (2008). A review of the main parameters influencing long-term performance and durability of PEM fuel cells. *Journal of Power Sources*, 180, 1–14.